

29 Mar 2001, 7:30 pm - 9:30 pm

## Evaluation of Site Response Using Downhole Array Data from a Liquefied Site

Zhi-Liang Wang

*Geomatrix Consultants, Inc., Oakland, CA*

C.-Y. Chang

*Geomatrix Consultants, Inc., Oakland, CA*

Chin Man Mok

*Geomatrix Consultants, Inc., Oakland, CA*

Follow this and additional works at: <https://scholarsmine.mst.edu/icrageesd>



Part of the [Geotechnical Engineering Commons](#)

### Recommended Citation

Wang, Zhi-Liang; Chang, C.-Y.; and Mok, Chin Man, "Evaluation of Site Response Using Downhole Array Data from a Liquefied Site" (2001). *International Conferences on Recent Advances in Geotechnical Earthquake Engineering and Soil Dynamics*. 24.

<https://scholarsmine.mst.edu/icrageesd/04icrageesd/session04/24>



This work is licensed under a [Creative Commons Attribution-Noncommercial-No Derivative Works 4.0 License](#).

This Article - Conference proceedings is brought to you for free and open access by Scholars' Mine. It has been accepted for inclusion in International Conferences on Recent Advances in Geotechnical Earthquake Engineering and Soil Dynamics by an authorized administrator of Scholars' Mine. This work is protected by U. S. Copyright Law. Unauthorized use including reproduction for redistribution requires the permission of the copyright holder. For more information, please contact [scholarsmine@mst.edu](mailto:scholarsmine@mst.edu).

# EVALUATION OF SITE RESPONSE USING DOWNHOLE ARRAY DATA FROM A LIQUEFIED SITE

Zhi-Liang Wang, C.-Y. Chang and Chin Man Mok  
Geomatrix Consultants, Inc.  
2101 Webster Street  
Oakland, California 94612-3027

## ABSTRACT

Downhole array ground motions recorded at Port Island during the mainshock and aftershocks of the Hyogoken-Nanbu (Kobe) earthquake of January 17, 1995, were used in this study for evaluating the reasonableness of commonly used site response analysis techniques (both nonlinear effective stress and equivalent linear total stress techniques). The nonlinear effective stress analyses were performed using the computer code SUMDES; the equivalent linear total stress analyses were performed using the computer code SHAKE. Dynamic soil properties as well as other data for characterizing nonlinear stress-strain, cyclic strength, and pore pressure generation and dissipation of the Masado fill that liquefied during the mainshock of the Kobe earthquake were derived from published papers

## INTRODUCTION

Liquefaction-related damages are recognized as one of the major geohazards produced by strong earthquakes. Because of the complex nonlinear soil response and excess pore water pressure build-up under dynamic loading, the ground motion characteristics developed at liquefied sites during strong earthquakes are not well understood. On January 17, 1995, the Hyogoken-Nanbu (Kobe) earthquake ( $M_w$  6.9) caused extensive liquefaction, lateral spreading, and liquefaction-induced settlement at the reclaimed Port Island. The ground motion data recorded by a downhole array in Port Island provide invaluable information for studying the ground motion characteristics at liquefiable sites and for calibrating nonlinear effective stress models used in site response analyses for predicting liquefaction phenomena. A number of studies have been performed to use these data to infer the nonlinear stress-strain properties of the soils (primarily the Masado fills that liquefied during the earthquake). Some studies are focused on calibrating equivalent linear models used in site response analyses. Some site response studies were conducted to calibrate effective stress models.

The objective of this study (Wang et al., 1999) is to use the ground motion data recorded by the Port Island downhole array during the Kobe earthquake to examine the validity of two site response analysis procedures that have been used in the geotechnical engineering profession. One of them is based on an equivalent linear approach using the computer program

SHAKE (Schnabel et al., 1972). The other one is based on a nonlinear effective stress approach using the computer program SUMDES (Li et al., 1992). Due to page limitation, only the results of the non-linear effective stress analyses are presented herein.

## PORT ISLAND DOWNHOLE ARRAY AND SUBSURFACE CONDITIONS

Port Island is an artificial island southwest of the city of Kobe in Japan. The site is located about 5 km from a fault. Based on the aftershock zone of the Kobe earthquake, this fault is believed to have ruptured during the mainshock. In October 1991, the Development Division of Kobe City installed a downhole array on Port Island (Iwasaki and Tai, 1996). The array consists of accelerometers installed at the ground surface and at depths of 16, 32, and 83 m.

As shown in Fig. 1, the site is underlain by about 18 to 19 m of fill having blowcounts ranging from 2 to 7 at depths shallower than 14 m and from 2 to 17 at depths from 14 to 19 m (Iwasaki and Tai, 1996). The fill, which is called the Masado soil, is composed of decomposed granite, with about 5% fines, 55% gravel, and 40% sand (Ishihara et al., 1996). Immediately below the fill is an 8-m layer of soft alluvial clay that is underlain by alluvial and diluvial deposits of sand, gravelly sand, and clay to a depth greater than 85 m. The depth of the water table at the time of the Kobe earthquake is estimated to have been about 3 m. The surficial fill is believed to have liquefied during the mainshock of the Kobe earthquake, as

evidenced by the widespread sand boils observed on the island (Shibata et al., 1996).

## DYNAMIC SOIL PROPERTIES AND STRESS-STRAIN CHARACTERISTICS

Depending on the methods used, various soil parameters are needed to perform site response analyses. In this study, total stress analysis was performed by the computer program SHAKE using an equivalent linear approach. The parameters required by this approach include the low-strain shear modulus (or shear-wave velocity), the soil density, and the relationships describing the shear strain-dependency of the shear modulus and damping ratio. Effective stress analysis was performed by the computer program SUMDES using a nonlinear approach. This approach requires model-dependent parameters describing stress-strain characteristics

### Dynamic Soil Parameters for Equivalent Linear Method

In 1991, the shear- and compressional-wave velocities at the array site were measured by downhole geophysical methods (Iwasaki and Tai, 1996). These velocities, along with the soil profile, soil layering, and SPT N-values, are depicted on Fig. 1.

The shear modulus reduction curves and damping curves assumed for various types of soils at Port Island were selected based on the available data for similar soils. For the fill (Masado soil), the average curves proposed by Seed and Idriss (1970) for sands were used. For the alluvial sand, the upper-bound modulus and lower-bound damping curves proposed by Seed and Idriss (1970) were used. For the clayey soils, the curve published by Vuceti and Dobry (1991) for PI=30 to 50 was used.

### Stress-Strain Characteristics for Effective Stress Analysis Using SUMDES

Effective stress site response analysis using the program SUMDES is described in Li et al. (1992). Bounding surface hypoplasticity model for sand (Wang et al., 1990) was used in the program. Estimates of model parameters for various soil layers at the Port Island site are described below.

Ishihara et al. (1998) presented their laboratory test results for undisturbed and reconstituted samples of the Masado soil obtained from Port Island. Undrained monotonic tests were performed to obtain the effective stress path and steady state parameters (undrained strength and residual strength). For the undisturbed samples, the results of the consolidation tests were summarized by the following equation:

$$e_c - e_o = 0.03 - 0.04 \log p', p' > 10kP_a \quad (1)$$

where  $e_c$  = void ratio at consolidation,  $e_o$  = initial void ratio, and  $p'$  = effective vertical stress. The effective stress paths under triaxial compression and extension tests are presented in Fig. 2 for an initial confining pressure of 100 kPa. These data were used to calibrate model parameters for Masado fill as illustrated below.

In this study, a simplified version of the original bounding surface hypoplasticity model for sand was used to characterize the Masado soil. This is the model type 4 in the program SUMDES. There are 10 parameters required for each soil layer .

### Calibration of Bounding Surface Hypoplasticity Model Parameters

Friction Angle,  $\phi$ : Based on the results of undrained triaxial tests (Ishihara et al., 1998) on Masado soil, the friction angle was estimated to be 31 degrees (or  $M=1.24$ ). There are no strength parameters available for materials other than the Masado fill. For the sandy layer below the alluvial clay, the measured blowcounts have an average value of  $(N_1)_{60}$  of 16. Below this layer is a diluvial gravelly sand (depths of 33 to 60 m), which has blowcounts ranging from 9 to over 50. The estimated friction angle is 40 degrees. We applied the same constitutive model for sand to the alluvial and diluvial clays (depths of 19 to 27 m and 61 to 79 m). Because these clays are not liquefiable, the generation of pore water pressure is disabled in these layers. An equivalent friction angle of 30 degrees was assumed for both the alluvial and diluvial clays.

Shear Modulus Coefficient,  $G_o$ : The elastic (or maximum) shear modulus,  $G_{max}$ , was first calculated based on measured shear-wave velocity,  $V_s$ , using the following relationship:

$$G_{max} = \rho V_s^2 \quad (2)$$

And then, for each layer with a void ratio  $e_o$  and an effective mean pressure  $p'$ ,  $G_o$  was calculated from the following equation used in the model

$$G_{max} = G_o P_a \frac{(2.973 - e)^2}{1 + e} \sqrt{\frac{p}{P_a}} \quad (3)$$

where  $G_o$  = shear modulus coefficient, and  $P_a$  = atmospheric pressure.

Compressibility under Isotropic Virgin Loading,  $\lambda$ : For the Masado soil, based on Ishihara et al. (1998), the compression index,  $C_c$ , is 0.04, Eq.(1). In the model we used, the consolidation line was described by the following equation:

$$e_c = e_0 - 2\lambda (p'/p_a)^{0.5} \quad (4)$$

This equation was demonstrated to fit the consolidation lines of sandy soils better than using  $\log p'$  (Wang et al., 1987). Both curves (Eq.(10 and (4)) agree well in the mean pressure range up to 140 kPa, as encountered in the Masado fill at Port Island. Thus, a calibrated value of  $\lambda = 0.026$  was used in the analysis. Except for the Masado fill, no laboratory test results were available. Thus, for other materials, values of  $\lambda$  equal to  $10 \kappa$  were used in the analysis ( $\kappa$  is defined below).

Swelling or Rebound Index,  $\kappa$ : The parameter  $\kappa$  is related to settlement calculations if soils are loaded under undrained conditions and pore water pressures are generated and subsequently dissipated. The swelling index  $\kappa$  for sand has the same meaning as defined in the consolidation theory for clay, but it is difficult to measure by laboratory tests for sand. In this study, no laboratory test was available for the parameter  $\kappa$  of the Masado fill. It was demonstrated by Wang et al. (1987) that the ratio of  $\lambda/\kappa$  is about 2, and values of  $\kappa$  can be estimated if  $\lambda$  is known. On the basis  $\kappa = 0.01$  was estimated for the Masado fill for the settlement analysis.

For materials other than the Masado fill, values of  $\kappa$  were estimated based on the following relationship with a Poisson's ratio of  $\nu$ :

$$\kappa = \frac{3(1 + e_0)^2 (1 - 2\nu)}{2G_0 (2.973 - e_0)^2 (1 + \nu)} \quad (5)$$

In this study, a  $\nu$  value of 0.03 was used for materials other than Masado fill.

Shear Stress versus Shear Strain,  $h_r$ : Parameter  $h_r$  characterizes the relationship between the magnitudes of the shear modulus and shear strain and was calibrated against a given shear modulus reduction curve  $G/G_{max}$ , which is the basic information used for performing equivalent linear analysis.

Phase Transformation Line,  $M_p$ : The phase transformation line (point) was defined for sandy soils to represent the stress state at which contractive behavior changes to dilative behavior under undrained shear loading. As shown in Fig. 3, for the Masado fill the contractive behavior transforms to dilative behavior when the stress ratio is greater than  $M_p = 1.03$ . For other materials, the phase transformation line was assumed to follow  $M_p/M = 0.75$ .

Effective Stress Path – Parameters  $k_r$  and  $b$ : Parameters  $k_r$  and  $b$  define effective stress paths, as described in Wang et al. (1990). Effective stress paths under undrained shear loading for Masado fill are shown in Fig. 2 (Ishihara, 1998). These stress paths are for triaxial compression and triaxial extension

only. Shown in Fig. 3 is a model prediction under simple shear conditions using parameters  $k_r = 0.15$  and  $b = 1.0$ . By varying  $k_r$  values, effective stress paths for different confining pressures representing Masado soil layers at 4 and 8 m depth were also estimated (Fig. 5). Assuming a variation of parameter  $k_r$ , similar effective stress paths were determined for each of the finite element layers in the fill. Using only one set of parameters for the Masado fill is possible (Wang et al., 2000) but it requires a complete information of the critical-state line.

For the sandy layer below the first clay layer underneath the fill, a higher  $k_r$  value was estimated, because this layer is denser than the fill. For other layers,  $k_r = 100$  was assumed, reflecting no generation of excess pore water pressure.

Pore Pressure Generation Due to Cyclic Loading,  $d$ : The parameter  $d$  is the pore water pressure generation parameter. For the Masado fill, cyclic strength data (in terms of cyclic stress ratio versus cycle number) are available. These data were used to calibrate model parameters for the liquefaction assessment of the Masado fill. Model predictions for effective stress paths using  $d=7$  are presented on Fig. 6 for stress ratios of 0.2. The model predictions of the number of cycles to liquefaction for different stress ratios are superimposed on data from Nagase et al. (1995) in Fig. 4.

The first sandy layer below the fill and clay layer is also susceptible to liquefaction (with an average blowcount of  $(N_1)_{60} = 16$ , denser than the Masado fill). Values of  $d=6$  to 10 were estimated for that layer. For other nonliquefiable layers,  $d = 100$  was assumed, reflecting no generation of excess pore water pressure.

## AVAILABLE RECORDINGS

As described previously, the accelerometers at the Port Island downhole array were installed on the ground surface and at depths of 16, 32, and 83 m. These accelerometers were synchronized and oriented in the N00E, N90E, and vertical directions. The array recorded the ground motions during the mainshock and aftershocks of the Hyogoken-Nanbu (Kobe) earthquake of January 17, 1995 ( $M_w$  6.9). Peak accelerations recorded at 83-m depth were 678.6 and 302.6 gals for the two horizontal components and 186.6 gals for the vertical component of the mainshock. These recordings were made available for this study through Geo-Research Institute, Osaka Soil Test Laboratory, Osaka, Japan.

The mainshock data used in this study was corrected by NKK of Japan. A number of researchers have noted that the vertical component of the motion recorded at a depth of 16 m during the mainshock contains some high peaks due to electronic noises (Shibata et al., 1996). These high peaks were removed in this study to allow comparison with the computed motions.

## SITE RESPONSE ANALYSIS USING SUMDES

As described previously, widespread liquefaction occurred at the Port Island downhole array site during the Kobe earthquake of January 17, 1995. Site response analyses using nonlinear effective stress analysis techniques, which have been used in the geotechnical engineering profession for site effect studies, were performed to evaluate the reasonableness of these techniques for predicting ground motion at sites that exhibit strong nonlinear soil response, including liquefaction phenomena. Analyses were performed for the mainshock (January 17, 1995). Input motions to these analyses are the motions recorded at a depth of 83 m. The recorded horizontal and vertical motions at depth of 83 m are presented in Fig. 5. Motions computed at depths of 0, 16, and 32 m were compared with the recorded motions. Both horizontal and vertical components were analyzed.

For the three-directional excitation, comparisons of acceleration time histories and response spectra (5% damped) of the computed and recorded motions are shown in Fig. 6 through 11. Induced peak pore water pressure profiles are shown in Fig. 12. Time histories of effective mean pressure computed at depths of 6, 12, 16, and 32 m are shown in Fig. 13. Figure 14 shows that the excess pore water pressures were dissipated 4 hours after the earthquake. The computed settlement profile after dissipation of excess pore water pressure is shown in Fig. 15. The computed settlement of 0.4 m at the ground surface is reasonable compared to the observed settlement of 0.2 to 0.5 m at Port Island (Shibata et al., 1996; Ishihara et al., 1996).

## SUMMARY AND CONCLUSIONS

Downhole array ground motions recorded at Port Island during the mainshock and aftershocks of the Hyogoken-Nanbu (Kobe) earthquake of January 17, 1995, were used in this study to evaluate the reasonableness of commonly used site response analysis techniques (both nonlinear effective stress and equivalent linear total stress techniques). The nonlinear effective stress analysis was performed using the computer code SUMDES. Dynamic soil properties as well as other data for characterizing nonlinear stress-strain, cyclic strength, and pore pressure generation and dissipation of the Masado fill that liquefied during the mainshock of the Kobe earthquake were derived from available publications.

The results of the nonlinear effective stress analysis show that the bounding surface hypoplasticity soil model implemented in SUMDES appears capable of predicting horizontal ground motions at the Port Island site that liquefied during the Kobe earthquake. Although the SUMDES program predicted reasonably well the vertical motion up to initiation of liquefaction, after that time the vertical motion computed is in poor agreement with the recorded motion.

The results of the equivalent linear total stress analysis (not presented in this paper) show that the horizontal motion computed by SHAKE is in a reasonable agreement with the recorded motion up to the time of initial liquefaction. As expected, the motion computed using the equivalent linear technique after liquefaction is in poor agreement with the recorded motion.

## ACKNOWLEDGMENTS

The Port Island downhole array data were provided by the Committee of Earthquake Observation and Research in the Kansai Area (CEORKA), Japan. Mr. Y. Iwasaki assisted in acquiring the aftershock data used in this study. Professor Ishihara kindly provided unpublished data on behavior of the Masado soil. Professor X.-S. Li gave valuable suggestions in modeling using SUMDES. Financial support for this study was awarded by the U.S. Geological Survey, Department of the Interior, under USGS award number (Geomatrix Consultants, Inc., 1434-HQ-97I-GR-02981). The views and conclusions contained in this document are those of the authors.

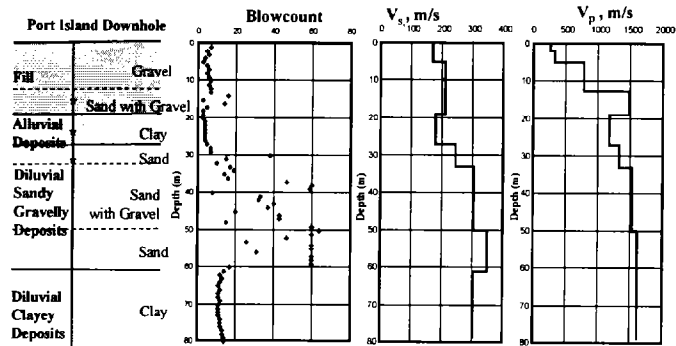
## REFERENCES

- Ishihara, K., Cubrinovski, M., and Nonaka, T., [1998]. "Characterization of Undrained Behaviour of Soils in the Reclaimed Area of Kobe." *Soils and Foundations*, Japanese Geotechnical Society, September.
- Iwasaki, Y., and Tai, M., [1996]. "Strong Motion Records at Kobe Port Island." *Special Issue of Soils and Foundations*, Japanese Geotechnical Society, January.
- Li, X.-S., Wang, Z.-L. and Shen, C. K., [1992]. "SUMDES, a Nonlinear Procedure for Response Analysis of Horizontally-layered Sites Subjected to Multi-directional Earthquake Loading." Report to Department of Civil Engineering, University of California, Davis.
- Schanberl, P.B., Lysmer, J., and Seed, H.B., [1972]. "SHAKE: A Computer Program for Earthquake Response Analysis of Horizontally Layered Sites." Report No. UCB/EERC-72/12, Earthquake Engineering Research Center, University of California, Berkeley, December, 102 p.
- Shibata, T., Oka, F., and Ozawa, Y., [1996]. "Characteristics of Ground Deformation due to Liquefaction." *Special Issue of Soils and Foundations*, Japanese Geotechnical Society, January.
- Wang, Z.L., Dafalias, Y.F., and Shen, C.K., [1987]. "Simulation and Prediction of Sand Behavior Using the Bounding Surface Hypoplasticity Model." *Proceedings of International Workshop on the Constitutive Equations for Granular Non-Cohesive Soils*, Cleveland, Ohio.

Wang, Z. L., Dafalias, Y. F., and Shen, C. K., [1990]. "Bounding Surface Hypoplasticity Model for Sand." *Journal of Engineering Mechanics*, ASCE, Vol. 116, No. 5. P.984-1001.

Wang, Z.L., Chang, C.Y., Mok, C.M., [1999]. "Evaluation of Site Response Using Downhole Array Data from a Liquefied Site." Award Number: 1434-HQ-97-GR-02982, FY 1997 NEHRP.

Wang, Z.L., Dafalias, Y.F., Li, X.S. and Makdisi, F.I., [2000]. "State Pressure Index for Modeling Sand Behavior." Submitted to ASCE for publishing.



\* Location of Downhole Instruments (at depths of 0, 16, 23, 32, and 83 m)

Fig. 1. Soil and Wave Velocity Profiles at Port Island Downhole Array Site (After Iwasaki and Tai, 1996)

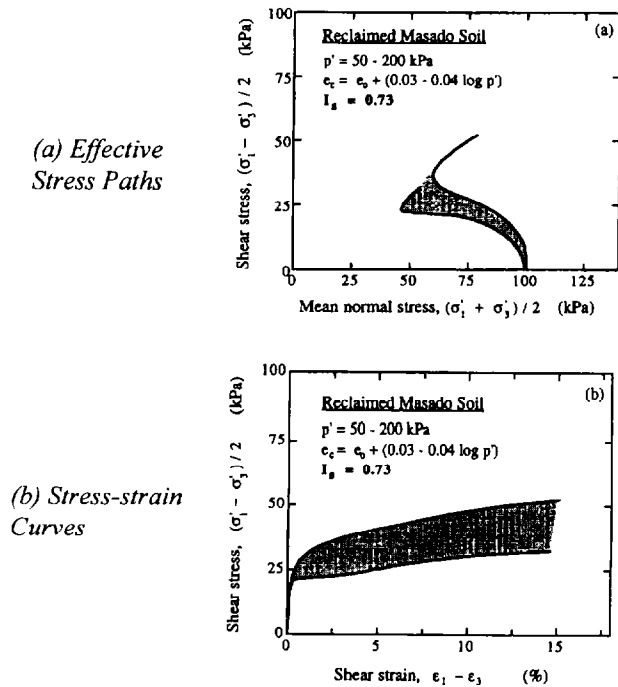


Fig. 2. Undrained Behavior of In-situ Masado Soils in Untreated Area (After Ishihara et al., 1998)

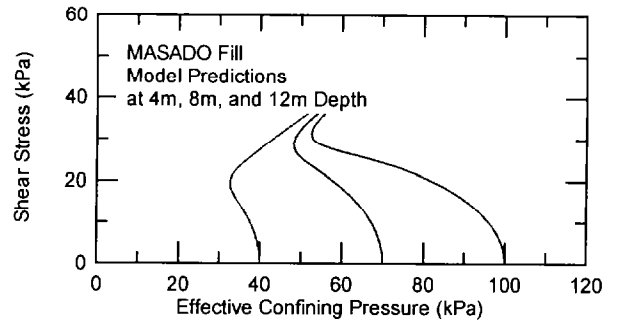


Fig. 3. Computed Effective Stress Paths for Masado Fill at Different Depths

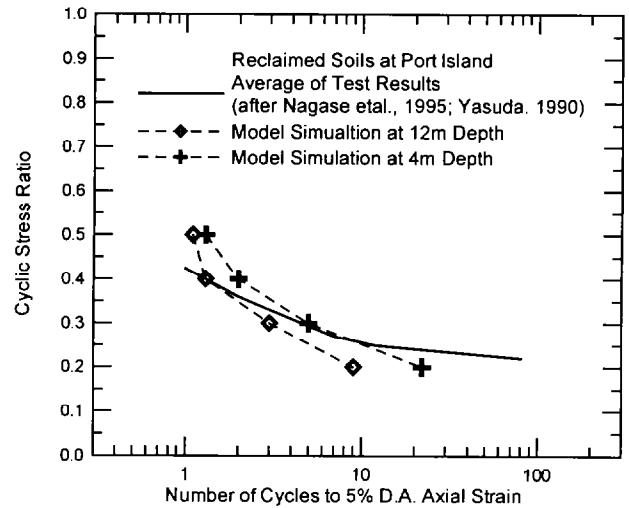


Fig. 4. Comparison of Model Simulation and Test Results for Cyclic Resistance to Liquefaction of Masado Fill

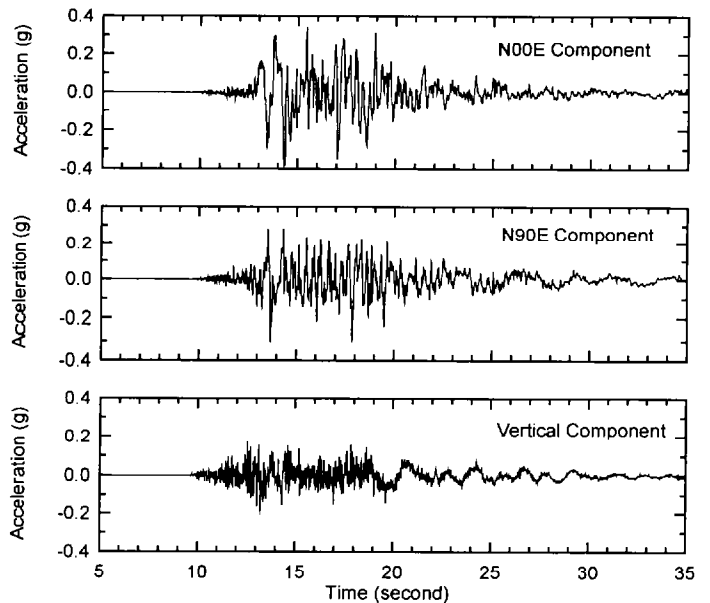


Fig. 5. Recorded Acceleration Time Histories at Depth 83m During 1995 Hyogoken-Nanbu Earthquake (after CEORKA)

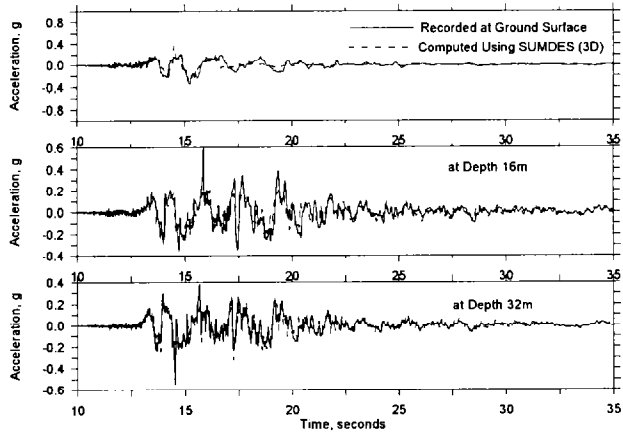


Fig. 6. Comparison of Recorded and Computed Acceleration Time Histories, N00E Component

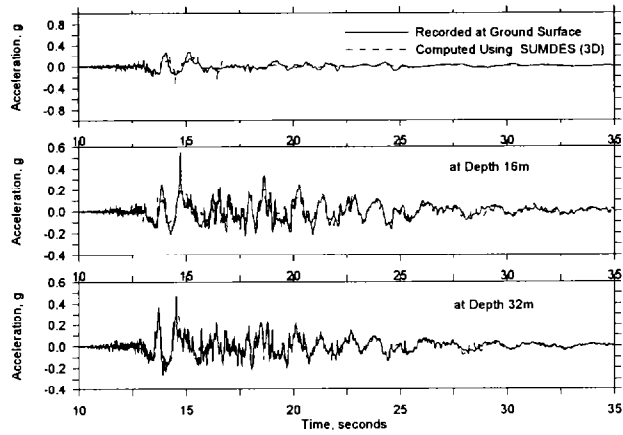


Fig. 7. Comparison of Recorded and Computed Acceleration Time Histories, N90E Component

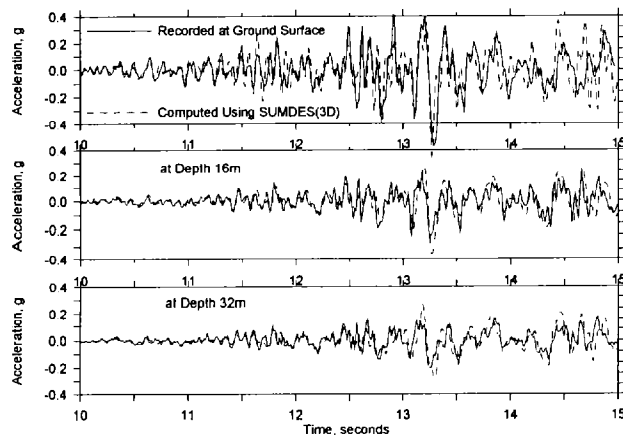


Fig. 8. Comparison of Recorded and Computed Acceleration Time Histories, Vertical Component (First 15 seconds)

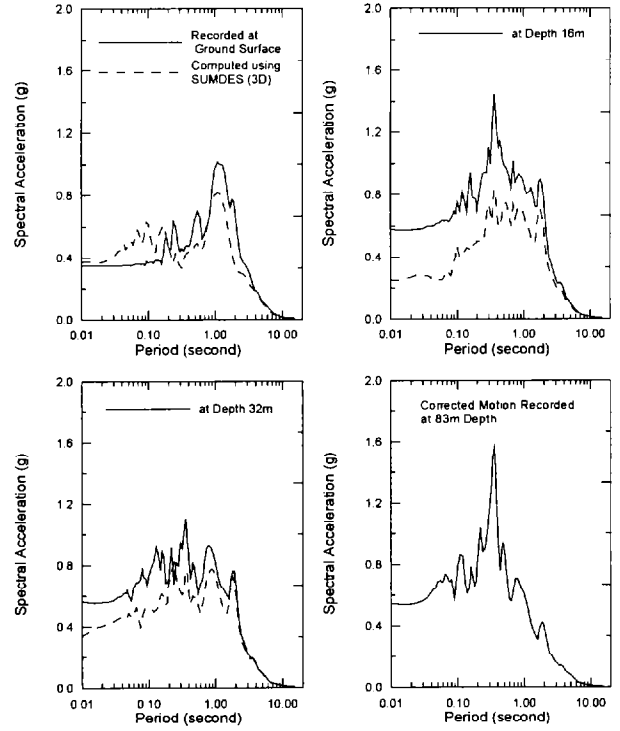


Fig. 9. Comparison of Response Spectra of Computed and Recorded Motions, N00E Component

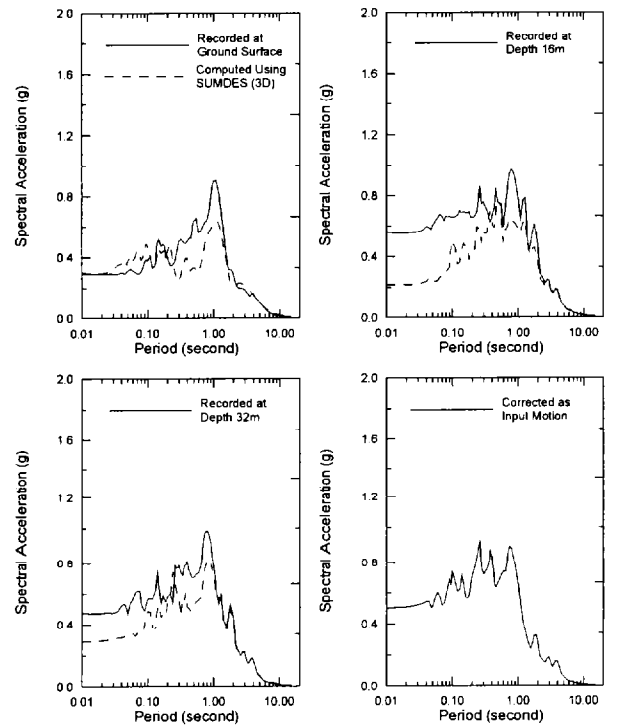


Fig. 10. Comparison of Response Spectra of Computed and Recorded Motions, N90E Component

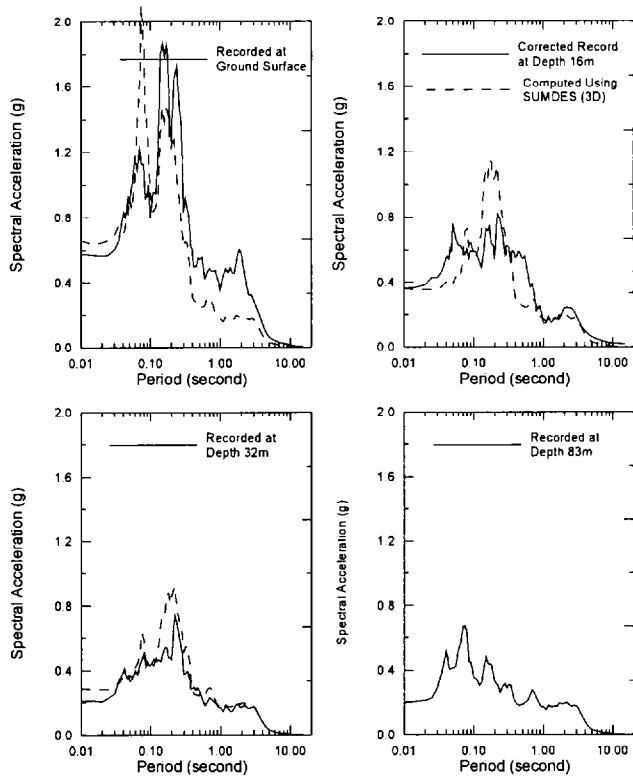


Fig. 11. Comparison of Response Spectra of Computed and Recorded Motions, Vertical Component

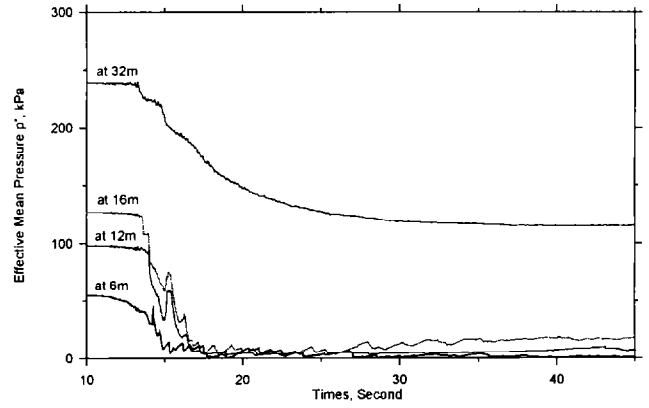


Fig. 13. Time Histories of Effective Mean Pressure  $p'$  Computed Using SUMDES

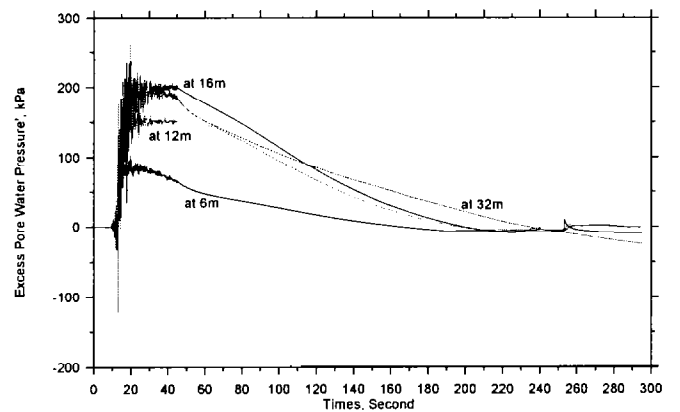


Fig. 14. Time Histories of Excess Pore Water Pressure Computed Using SUMDES

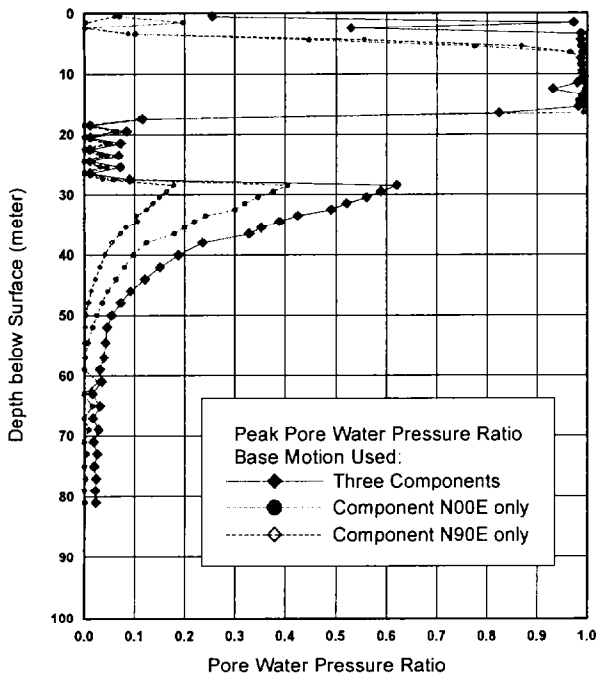


Fig. 12. Variation of Induced Peak Pore Water Pressure Ratio with Depth

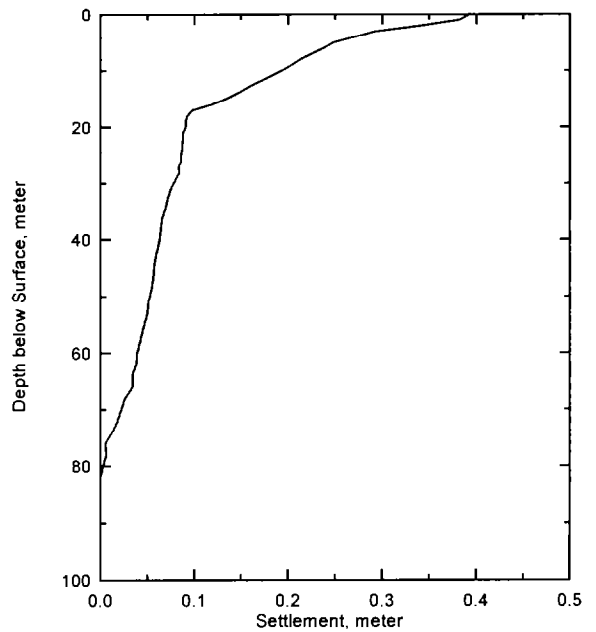


Fig. 15. Computed Settlement Profile at Port Island Downhole Array